

# Color and Texture Based Segmentation of Molecular Pathology Images using HSOMs

Manasi Datar<sup>1</sup>, Dirk Padfield<sup>2,3</sup>, and Harvey Cline<sup>2</sup>

<sup>1</sup>GE Global Research, Hoodi Village, Whitefield Road, Bangalore, India

<sup>2</sup>GE Global Research, One Research Circle, Niskayuna, NY, 12309

<sup>3</sup>Rensselaer Polytechnic Institute, 110 8th St., Troy, NY 12180

**Abstract**—Prostate cancer is the most common cancer among men, excluding skin cancer. It is diagnosed by histopathology interpretation of Hematoxylin and Eosin (H&E)-stained tissue sections. Gland and nuclei distributions vary with the disease grade, and the morphological features vary with the advance of cancer. A tissue microarray with known disease stages can be used to enable efficient pathology slide image analysis. We focus on an intuitive approach for segmenting such images, using the Hierarchical Self-Organizing Map (HSOM). Our approach introduces the use of unsupervised clustering using both color and texture features, and the use of unsupervised color merging outside of the HSOM framework. The HSOM was applied to segment 109 tissues composed of four tissue clusters: glands, epithelia, stroma and nuclei. These segmentations were compared with the results of an EM Gaussian clustering algorithm. The proposed method confirms that the self-learning ability and adaptability of the self-organizing map, coupled with the information fusion mechanism of the hierarchical network, leads to superior segmentation results for tissue images.

## I. INTRODUCTION

Prostate cancer is the most common cancer among men, excluding skin cancer. The American Cancer Society estimates over 220,000 new cases of prostate cancer and nearly 30,000 deaths in the United States per year. A prostate cancer diagnosis is typically established by histopathology using Hematoxylin and Eosin (H&E)-stained tissue sections [1], and pathologists use human pattern recognition to grade prostate cancer. Digital microscopy is becoming increasingly popular in pathology, and morphology from H&E slides obtained with image processing has been correlated with cancer [2], [3], [4]. Tissue microarrays (TMA) are used for high-throughput pathology research wherein multiple tissues are simultaneously processed to remove staining variability and to reduce labor. The tissue cores from different patients are embedded in a paraffin block and sliced to give multiple registered arrays. TMAs are used in drug discovery to test the protein expression in tissues with a range of known outcomes [5].

Computer vision methods are not yet used in clinical practice in relation to digital pathology. A first step is segmentation of the image into different tissue types, which enables the detection of abnormal regions in a pathology slide since cancer involves abnormal morphology that is difficult to quantify. It provides information that would be tedious to obtain manually such as counting nuclei. Any survey of image segmentation methods, such as [6], usually includes

edge detection, region growing, region splitting and merging, histogram thresholding and clustering. Edge detection and histogram thresholding methods work well with gray level images, but they are not suitable for color images as color components are interdependent and should not be processed individually. Neighborhood-based methods, such as region growing/splitting, use only local information, while global methods like feature-space clustering do not take advantage of local spatial knowledge at all [7]. In contrast to these classical methods, the artificial neural network (ANN) approach has the advantages of parallel processing (with appropriate hardware), robustness, noise tolerance, and adaptability.

Hierarchical Self-Organizing Maps (HSOM) provide a framework for unsupervised clustering. This provides a unique advantage by making the algorithm robust to missing data. In this paper, we propose a method for segmentation of glands, nuclei, epithelial tissue, and stroma from molecular pathology images using a 2-stage HSOM.

The application of learning paradigms such as the HSOM is sparse in the field of color image segmentation. Our approach leverages the unique advantages of the HSOM including unsupervised clustering, along with the use of multi-spectral features including texture. The region merging step increases discrimination between clusters and similarity within a cluster. Being unsupervised, our method requires no *a priori* knowledge about the image being segmented. It uses information within the given image to identify dominant clusters (segments). As such, it is also robust in case of missing/variable number of segments. With relevant *a priori* knowledge, recognition may also be carried out in the same framework (e.g. differentiate cancer cells from normal cells). The quality of segmentation using ANNs is dependent on the granularity of the neuron combinations, and often results in over-segmentation. Supervised region merging carried out on the resultant topological map to optimize segmentation defeats the purpose of the unsupervised training phase. We implement the concept of neuron-merging, which finds neurons with similar states (prototype vectors) in the topological map resulting from the HSOM, and merges them to optimize the segmentation further.

In Section II, we describe our formulation of HSOMs as applied to microscopy images. In Section III, we demonstrate qualitative results of the HSOM relative to EM Gaussian clustering. And in Section IV, we state our conclusions and steps for future work.

## II. METHODS

The flowchart in figure 1 describes the various stages in the segmentation process using HSOMs. The elements of the flow chart are described in the following subsections.

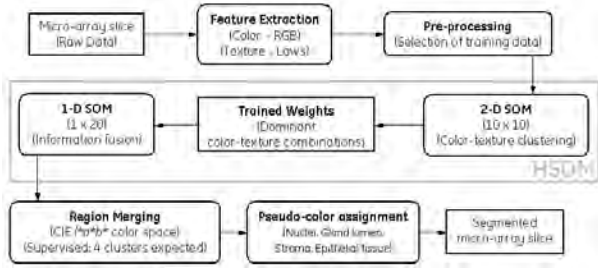


Fig. 1. Flowchart of the proposed method.

### A. Feature Extraction

Each pixel is represented as a 7-dimensional vector  $\{R, G, B, E5'L5, E5'S5, R5'R5, L5'S5\}$  of features suitable for training and subsequent classification using the HSOM.

The first three components of the feature vector are R, G, B values for every pixel in the image. There have been efforts to distinguish stain colors using an unmixing algorithm such as [8]. While such algorithms help in quantification and also to compute statistical metrics such as one required for image registration, they may not aid segmentation. The nonlinear nature of the RGB color space introduces interdependence between the channels and any such relationship - reflected in the combination of R, G, B values for a particular tissue type, from a particular acquisition - will provide important information for the classifier. Hence we retain this color space for feature extraction.

The next four components are texture features obtained by applying Laws' filters. Laws [9] developed a set of two-dimensional masks derived from five simple one-dimensional filters. They are  $L5 = [1 \ 4 \ 6 \ 4 \ 1]$ ,  $E5 = [-1 \ -2 \ 0 \ 2 \ 1]$ ,  $S5 = [-1 \ 0 \ 2 \ 0 \ -1]$ ,  $W5 = [-1 \ 2 \ 0 \ -2 \ 1]$ , and  $R5 = [1 \ 4 \ 6 \ -4 \ 1]$ . The mnemonics stand for Level, Edge, Spot, Wave and Ripple. Laws convolved these masks with the transposes of each other to provide a set of symmetric and anti-symmetric center-weighted masks. A Principal Component Analysis (PCA) revealed four masks [9] which significantly capture the underlying texture:  $E5'L5$ ,  $E5'S5$ ,  $R5'R5$ ,  $L5'S5$ . These masks are convolved with the original image to produce four corresponding feature images, which estimate the energy within the pass-band of their associated filters. Thus, Laws' texture energy transforms are a class of spatial-statistical transforms that effectively discriminate among texture fields. The essence of this approach is local measurement of the energy passed by a set of symmetric and anti-symmetric filters. The choice is justified by the fact that the local convolution approach used by Laws is computationally simpler as compared to frequency domain texture filters and is also found to be adequate for the application.

The image is convolved with each of the four masks to obtain corresponding texture energy images. These provide a

4-component texture feature vector for every pixel. Assuming that the image has  $R$  rows and  $C$  columns, the input to the 2-D SOM is a matrix of feature values for all the pixels in the image, formulated as a  $7 \times (R \times C)$  matrix.

### B. Hierarchical Self-Organizing Map

The hierarchical self-organizing map (HSOM) is a variant of the self-organizing map (SOM), proposed by Kohonen [10]. A SOM usually consists of  $M$  neurons located on a regular 1- or 2-dimensional grid. Higher dimensional grids are generally not used as they are difficult to visualize. The training mechanism for the basic SOM is iterative. Each neuron  $i$  has a  $d$ -dimensional prototype vector  $\mathbf{m}_i = [m_{i1}, \dots, m_{id}]$ . At each training step, a sample data vector  $\mathbf{x}$  is randomly chosen from the training set. Distances between  $\mathbf{x}$  and all prototype vectors are computed. The best-matching unit (BMU), denoted here by  $b$ , is the map unit with prototype closest to  $\mathbf{x}$ :

$$\|\mathbf{x} - \mathbf{m}_b\| = \min_i \{\|\mathbf{x} - \mathbf{m}_i\|\} \quad (1)$$

Next, the prototype vectors are updated. The BMU and its topological neighbors are moved closer to the input vector. The update rule for the prototype vector of unit  $i$  is:

$$\mathbf{m}_i(t+1) = \mathbf{m}_i(t) + \alpha(t)h_{bi}(t)[\mathbf{x} - \mathbf{m}_i(t)], \quad (2)$$

where  $t$  denotes time,  $\alpha(t)$  is learning rate and  $h_{bi}(t)$  is a neighborhood kernel centered on the BMU. The learning rate  $\alpha(t)$  and neighborhood radius of  $h_{bi}(t)$  decrease monotonically with time. During training, the SOM behaves like a flexible net that folds onto the "cloud" formed by the training data. Because of the neighborhood relations, neighboring prototypes are pulled in the same direction, and, hence, prototype vectors of neighboring units resemble each other. Thus, the goal of an SOM is to create a topologically (i.e. locally) ordered mapping of the input data.

Experiments have shown that it is very difficult to extract dominant features accurately if only a one-dimensional SOM is used. In contrast, it is difficult to avoid over-segmentation if only a two-dimensional SOM is used. The hierarchical SOM (HSOM) can be defined as a two-layer SOM whose operating principle is:

- 1) For each input vector  $\mathbf{x}$ , the best matching unit is chosen from the first layer map, and its index  $b$  is input into the second layer;
- 2) The best matching unit for input  $b$  is chosen from the second layer map, and its index is the output of the network.

The advantage of using the HSOM is that each high dimensional data vector is mapped to a low-dimensional discrete value so that comparing the values implicitly contains comparison of the original distances.

For this specific application, the HSOM is used as a pixel classifier (i.e. no image level features are required for clustering). As such, a chosen subset of pixels from the image may be used to "learn" the underlying clusters, thereby obviating the need for a separate set of training images. Such pixels can be selected based on sub-image statistics as described in [11] or in a sequential/random manner from the entire image. Since it is

difficult for any training set to capture variation present across all combinations of tissue and pathology, such a method is advantageous as it captures the variation in individual images. The first layer consists of a 2D SOM network laid out as a 10x10 matrix, while the second layer is a 1D SOM with 20 neurons arranged linearly. The number of neurons were chosen after a set of empirical experiments to determine an optimal arrangement. In the Matlab implementation, prototype vectors for neurons in both layers are initialized to the mid-point of the respective input range.

### C. Region Merging

The output of the HSOM is, more often than not, an over-segmented image. The colors obtained at the end of HSOM testing stage can be perceived as labels assigned by the classification scheme. Conceptually, they are representations of neuron states, i.e. similar regions in the image correspond to neurons with similar prototype configurations (or states). Hence, such neurons can be merged to arrive at a perceptually consistent segmentation. This is achieved by a homogeneity-based region-merging algorithm similar to [12]. While [12] works with real color values in the image, we are looking to merge similar neurons based on the color characteristics learned by the network.

The RGB color space was used for feature extraction as it is simple to use and its nonlinear nature ensures that relationships between the various color channels are utilized in the classification process. However, this very characteristic can prove detrimental when used in a distance-based algorithm. Perceptually linear color spaces - where a change in color value is nearly equal in magnitude to a change in visual importance as perceived by humans - are desirable for such computation. Hence, the color characteristics of the neurons are transformed into the CIE ( $L^*a^*b^*$ ) color space for region merging.

Each of the  $k$  ( $k \leq 20$ ) colors (or labels) generated by the HSOM represents a region. The CIE ( $L^*a^*b^*$ ) color-difference is calculated for all pairs of labels ( $i$  and  $j$ ) according to the equation

$$\Delta E_{ij} = \sqrt{(\Delta L_{ij}^*)^2 + (\Delta a_{ij}^*)^2 + (\Delta b_{ij}^*)^2} \quad (3)$$

This results in a list  $d$  of  $\frac{k(k-1)}{2}$  color differences. The mean ( $\mu_d$ ) and standard deviation of this list ( $\sigma_d$ ) are used to compute the threshold for region merging as

$$T_d = \mu_d - \sigma_d \quad (4)$$

In the region-merging algorithm, two regions with the smallest color difference are located. If this difference is smaller than  $T_d$ , the two regions are merged. The label of the new region is calculated as the mean of the labels of its component regions. This process is continued till there are no pairs with a difference smaller than  $T_d$ . Alternately, if the number of underlying tissue types is known *a priori*, it can also be used as the stopping criteria.

Since we are looking for four classes (nuclei, stroma, epithelial tissue, and gland lumen), merging is carried out

TABLE I  
SAMPLED TISSUE VALUES FROM A NORMAL PROSTATE IMAGE IN TWO  
DIFFERENT TISSUE MICRO ARRAYS.

Tissue type	red	green	blue
Tissue Microarray (Cytomix)			
Gland Lumen	170 ± 4	174 ± 5	173 ± 5
Epithelia	139 ± 19	100 ± 20	129 ± 20
Stroma	139 ± 16	59 ± 13	83 ± 19
Nuclei	59 ± 14	38 ± 11	77 ± 10
Tissue Microarray (Imgenex)			
Gland Lumen	119 ± 2	113 ± 2	103 ± 3
Epithelia	112 ± 4	80 ± 10	81 ± 8
Stroma	108 ± 6	65 ± 6	63 ± 8
Nuclei	52 ± 14	26 ± 10	43 ± 10

until we have four clusters left. The segmented image thus generated is seen to have more homogeneity within the regions and more disparity between them. Finally, the segmented image is recolored for ease of visualization using the following mapping: nuclei (blue), stroma (red), epithelial tissue (pink), and glands (white).

### III. RESULTS

Prostate cancer TMAs were obtained from Cytomix and Imgenex containing a total of 109 tissue elements consisting of both human prostate cancer and normal controls. H&E stained slides of size 1024\*768 were acquired using a 10X objective with a white light microscope (Leica) stored as 24 bit RGB files for image processing. The tissue microarray elements were digitized and processed to segment the different tissue compartments. A normal prostate tissue image at 10X shows glands with an epithelial layer and nuclei arranged along the boundary and stroma in the interior.

The cell nuclei have a dark color due to the Hematoxylin stain. The stroma contains smooth muscle cells and fibroblasts and stains red by Eosin. There is a slight difference between the epithelial tissue and stroma. The glands are epithelial tissue that is lightly stained by Eosin. The gland lumen does not contain tissue and has the same color as the background.

The manual segmentation of the four tissues is extremely time intensive. Moreover, for meaningful comparison, the manual analysis should be done by an expert pathologist, whose time is extremely valuable. Alternatively, an overall score can be reported by the pathologist, and this can be compared to some measure derived from the segmentation result. For example, the slides were documented with Gleason score and tumor staging information. The Gleason grading system is conducted by observing five selected gland patterns, and adding the two most significant pattern scores to give a score from two to ten [13]. The tumor staging is grouped into five categories, 1) Normal 2) T1 Nx Stage I Adenocarcinoma, 3) T1 Nx Stage II, 4) Stage III and 5) Stage IV. The full tissue array and segmentation along with the corresponding Gleason and tumor staging scores are not given here due to space constraints. Because this work focuses on the segmentation step, the use of such measures is a topic for future work.

Here we present qualitative comparisons of the results of the HSOM to the clustering method using EM Gaussian clustering

initialized with a K-means algorithm. To initialize the K-means clusters, regions of interest were manually selected in the gland lumen, epithelial tissue, stroma and nuclei, and the average intensity in each RGB channel was measured; these values are shown in Table I.

Each tissue sample may have different cluster centers because the intensity of the illumination changes from one image to the next, so an iterative K-means procedure is used for each image in the series to find more accurate cluster centers after initialization with the measured average intensity. K-means [14] is a robust segmentation algorithm that uses distances to the cluster centers to label the tissues. The sample pixel vectors  $x_i$  in RGB space are labeled by the closest Euclidean distance to the trial mean of the  $m^{\text{th}}$  tissue type,

$$\text{label}_i = \arg \min_m |\mu_m - x_i|. \quad (5)$$

The estimation of the mean vector

$$\mu_m = \frac{1}{N_m} \sum_{i \in m} x_i \quad (6)$$

is iterated to improve the segmentation, where  $N_m$  is the number of samples with the label  $m$ . Each RGB pixel in the image is then labeled by the closest tissue type cluster center in Euclidean 3D color space.

The EM Gaussian algorithm [15], [16] is a maximum likelihood algorithm where the clusters are fit to a mixture of Gaussians wherein the most likely tissue is used to segment the image. Using the initialization from the K-means, a further improvement is estimating the mean  $\mu_m$  and covariance  $\Sigma_m$  to fit a mixed Gaussian distribution to the sampled pixels. The mean and covariance are estimated by a mixture of Gaussians of the form

$$p(x_i, \mu_m, \Sigma_m) = \frac{1}{\sqrt{2\pi^K |\Sigma_m|}} \exp\left(-\frac{(x_i - \mu_m)^T \Sigma_m^{-1} (x_i - \mu_m)}{2}\right) \quad (7)$$

that approximates the  $m^{\text{th}}$  cluster distribution. Here  $K = 3$  since the distribution is 3-dimensional with RGB. Then Bayes' rule gives

$$P_m(x) = \frac{a_m p(x_i, \mu_m, \Sigma_m)}{\sum_{m=1}^M a_m p(x_i, \mu_m, \Sigma_m)} \quad (8)$$

where  $P_m(x_i)$  is the probability of observing class  $m$  given the observed data and the parameters (*a posteriori*). Here the mixture weight  $a_m$  is estimated numerically with  $\mu_m$  and  $\Sigma_m$  [17], [2]. The coefficients are found by iterating

$$a_m = \frac{\sum_{i=1}^N P_m(x_i)}{N} \quad (9)$$

$$\mu_m = \frac{\sum_{i=1}^N x_i P_m(x_i)}{\sum_{i=1}^N P_m(x_i)} \quad (10)$$

$$\Sigma_m = \frac{\sum_{i=1}^N P_m(x_i) (x_i - \mu_m)(x_i - \mu_m)^T}{\sum_{i=1}^N P_m(x_i)} \quad (11)$$

Using the EM Gaussian algorithm, the image is labeled by the maximum tissue probability.

Examples of the EM Gaussian segmentation for different cancer stages are shown in the middle column of Figure 2. The results of HSOM segmentation are shown in the right column of Figure 2. The first and third rows give examples of normal tissues, and the second and fourth rows give examples of various tumor stages.

The HSOM results demonstrate that the nuclei and gland segmentation are similar to the EM Gaussian method. However, the distribution is different for the epithelial and stroma tissues, which are spectrally the most similar classes. Whereas the EM Gaussian method tends to classify more regions as stroma, the HSOM algorithm is better able to separate these two tissues through the use of texture features in addition to spectral features.

The EM Gaussian method tends to produce fragmented segments as variation about individual cluster centers is not adequately modeled during training. The HSOM classification has more discrimination. The neuron-merging stage ensures increased homogeneity within individual segments and also provides better discrimination between different segments. This observation also emphasizes the advantage derived by using pixels from the available image for training, as opposed to an extensive set of training images. This is a significant advantage as it is difficult to compose a training set which captures all the variations occurring in clinical data.

Finally, the neuron configurations at the end of the segmentation procedure are prototype color-texture combinations for the tissue types present in that image. These can further be used in the recognition and annotation of tissue types, leading to further automation of image analysis processes.

Figure 3 shows the original tissue array of the 49 Imgenex tissues along with the HSOM segmentation. Table II lists the corresponding Gleason and tumor staging scores.

#### IV. CONCLUSIONS AND FUTURE WORK

We have presented a method using HSOMs for segmenting H&E prostate TMAs into tissue compartments. Our approach introduces several steps that improve the quality of the segmentation. The proposed two-stage hierarchical approach based on the self-organizing map combines the advantages of unsupervised learning based on large datasets and labeling of the clustered outputs. The network detects the dominant color and texture features in a given color image. These are subsequently used to segment the image by pixel classification. We compared the results of the HSOM to those obtained using an EM Gaussian mixture model. The use of texture in our model improves the ability of the algorithm to discriminate among the four classes in the images, especially between the epithelial and stroma tissues.

Future work includes extracting discriminate features from the segmentations that can be correlated with the Gleason and tumor staging scores. This will enable automatic staging of tissue images, which can then be used for training new pathologists and can serve as a second reader in the analysis of such images.

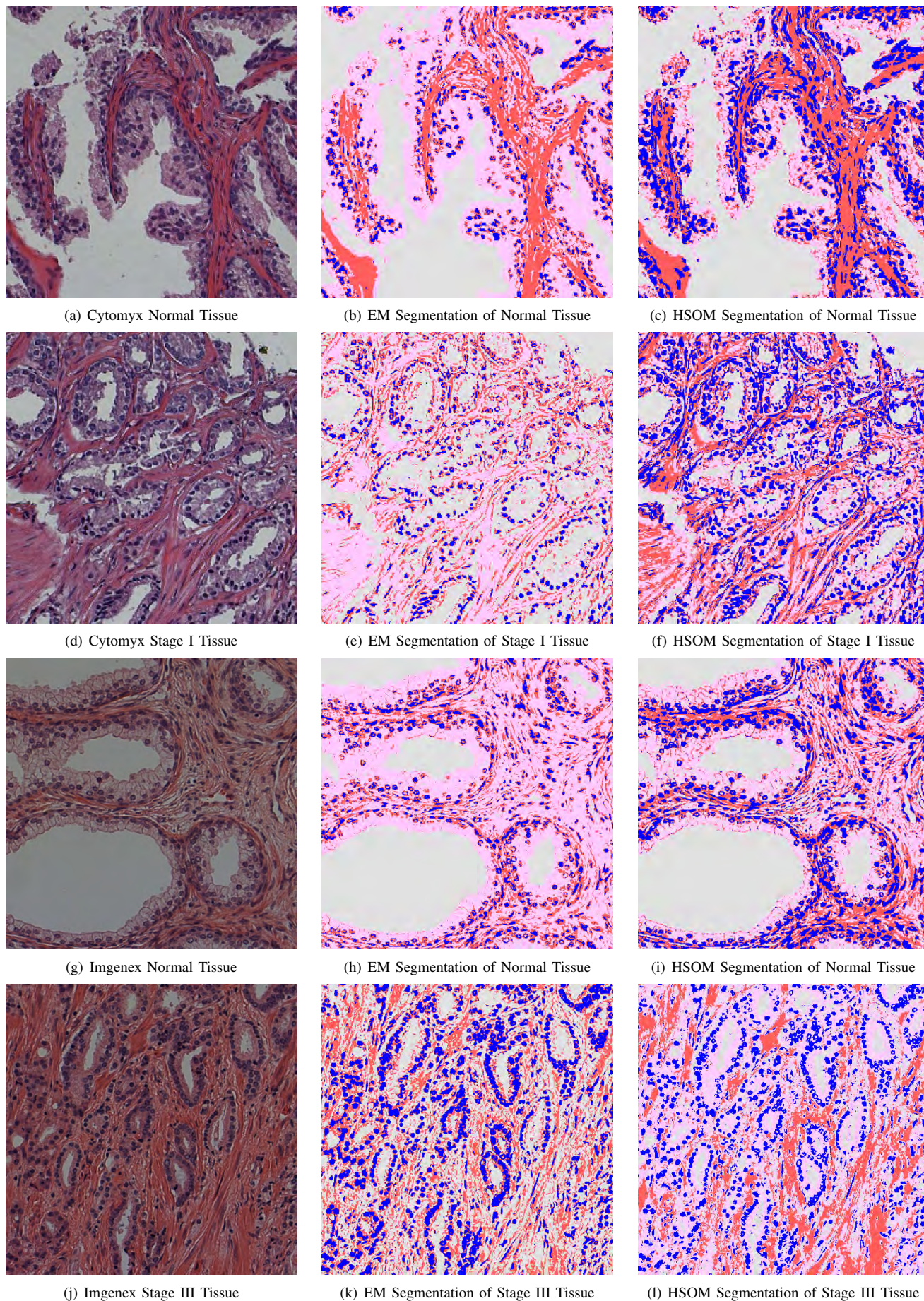


Fig. 2. Comparison of segmentation results on Cytomix and Imgenex datasets. The images in the left column are the original images, in the middle column are the EM segmentations, and on the right are the HSOM segmentations. Because of the use of texture, the HSOM method is better able to separate the spectrally similar stroma and epithelial tissues.

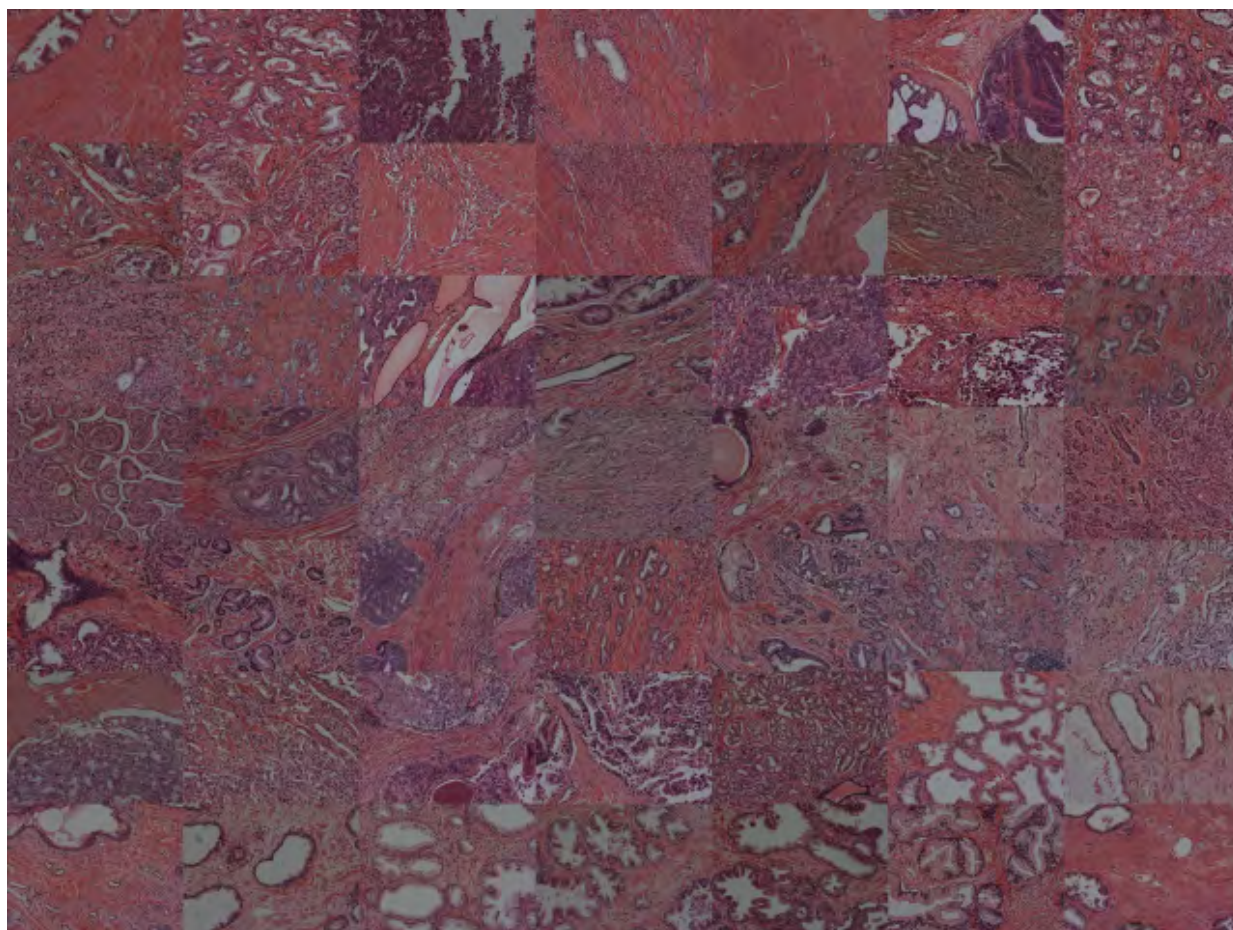
TABLE II

GLEASON AND TUMOR STAGING SCORES. THE FIRST NUMBER REPRESENTS THE GLEASON SCORE, AND THE SECOND NUMBER REPRESENTS THE TUMOR STAGING SCORE.

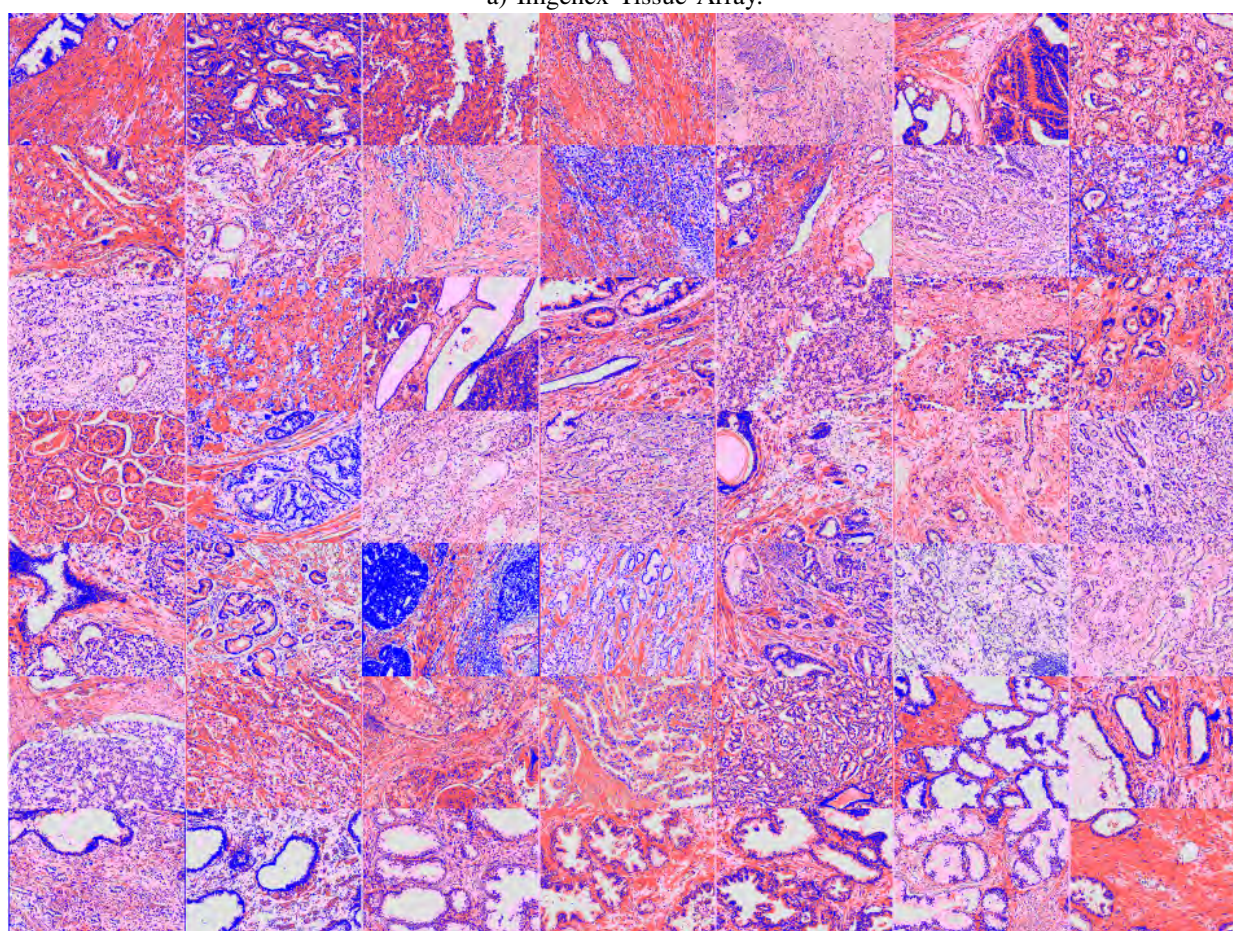
9, III	7, II	9, III	10, III	9, III	8, IV	7, II
7, II	7, II	9, III	9, III	7, III	7, IV	9, III
9, IV	7, III	9, IV	7, III	7, III	9, III	7, III
7, II	6, III	9, II	9, III	8, III	6, III	7, III
8, II	6, III	7, III	8, III	10, II	7, III	8, III
9, III	9, III	9, III	9, III	8, III	0, Normal	0, Normal
0, Normal	0, Normal	0, Normal	0, Normal	0, Normal	0, Normal	0, Normal

## REFERENCES

- [1] P.A. Humphrey, "Prostate pathology," *Chicago: American Society of Clinical Pathology*, 2003.
- [2] P.H. Bartels, T. Gahm, and D. Thompson, "Automated microscopy in diagnostic histopathology: From image processing to automated reasoning," *International Journal of Image Systems and Technology*, vol. 8, pp. 214–223, 1997.
- [3] P. Wolfe, J. Murphy, J. McGinley, Z. Zhu, W. Jiang, E.B. Gottschall, Henry, and H.J. Thompson, "Using nuclear morphometry to discriminate the tumorigenic potential of cells: A comparison of statistical methods," *Epidemiol Biomarkers Prev.*, vol. 13, no. 6, June 2004.
- [4] K. Huang and R.F. Murphy, "From quantitative microscopy to automated image understanding," *Journal of Biomedical Optics*, vol. 9, no. 5, pp. 893–912, 2004.
- [5] R.L. Camp, G.D. Chung GD, and D.L. Rimm, "Automated subcellular localization and quantification of protein expression in tissue microarrays," *Nature Medicine*, vol. 11, pp. 1323–1327, 2002.
- [6] H. D. Cheng, X. H. Jiang, Y. Sun, and J. L. Wang, "Color image segmentation: advances and prospects," *Pattern Recognition*, vol. 34, pp. 2259–2281, 2001.
- [7] R. Ohlander, K. Price, and D. R. Pierson, "Picture segmentation using a recursive region splitting method," *Computer Graphics and Image Processing*, vol. 8, pp. 313–333, 1978.
- [8] A. Rabinovich, S. Agarwal, C. A. Laris, J.H. Price, and S. Belongie, "Unsupervised color decomposition of histologically stained tissue samples," *Proceedings of Neural Information Processing Systems*, 2003.
- [9] K. I. Laws, "Texture energy measures," *Proceedings of Image Understanding Workshop*, pp. 47–51, November 1979.
- [10] T. Kohonen, "The self-organizing map," *Proceedings of the IEEE*, vol. 78, pp. 1464–1480, September 1990.
- [11] M. Datar, "Natural scene segmentation based on information fusion and hierarchical self-organizing maps," M.S. thesis, Utah State University, May 2005.
- [12] H. D. Cheng and Y. Sun, "A hierarchical approach to color image segmentation using homogeneity," *IEEE Transactions on Image Processing*, vol. 9, pp. 2071–2082, 2000.
- [13] D.F. Gleason, *Histologic grading of prostatic carcinoma*, New York: Churchill Livingstone, 1990.
- [14] J.A. Hartigan and M.A. Wong, "A k-means clustering algorithm," *Applied Statistics*, vol. 28, pp. 126–130, 1979.
- [15] A. P. Dempster, N.M. Laird, and D.B. Rubin, "Maximum-likelihood from incomplete data via the em algorithm," *J. Royal Statist. Soc. Ser. B.*, vol. 39, 1977.
- [16] R. Redner and H. Walker, "Mixture densities, maximum likelihood and the em algorithm," *SIAM Review*, vol. 26, no. 2, 1984.
- [17] M.A. Rubin, M.P. Zerkowski, R.L. Camp, R. Kuefer, M.D. Hofer, A.M. Chinnaiyan, and D.L. Rimm, "Quantitative determination of expression of the prostate cancer protein aal-methylacyl-coa racemase using automated quantitative analysis (aqua)," *American Journal of Pathology*, vol. 164, pp. 831–840, 2004.



a) Imgenex Tissue Array.



b) HSOM segmentation of the Imgenex Tissue Array.

Fig. 3. Tissue Array and corresponding HSOM segmentation.